JOURNAL OF APPLIED ELECTROCHEMISTRY 3 (1973) 17–22

Effects of mercury on the surfaces of polycrystalline copper, tin and zinc

R. BARNARD

The Ever Ready Co. (G.B.) Ltd., London, U.K.

Received 12 June 1972

Interfacial capacitance measurements have been used to study the effects of mercury on diamond polished copper, tin and zinc surfaces in 10M KOH. In the case of copper, microgram quantities of mercury were sufficient to inhibit the adsorption of hydrogen and reduce the surface heterogeneity. In contradistinction to copper, similar concentrations of mercury were found to increase the heterogeneity of tin and zinc surfaces. A decrease in surface heterogeneity for zinc was only observed at very high mercury concentrations. The increased surface heterogeneity is thought to arise from dissolution at the intercrystalline grain boundaries by mercury.

1. Introduction

The zinc electrode in a number of alkaline battery systems is amalgamated to improve both its discharge and corrosion characteristics [1]. Consequently this has necessitated a better understanding of the way in which mercury modifies the surface topography of polycrystalline zinc. Since few systematic double-layer studies have been reported for metals doped with small quantities of mercury it was considered worthwhile to compare the behaviour of zinc with other metals. Copper and tin were chosen for this study.

2. Experimental

2.1 *Instrumentation*

Capacitance measurements were made using a conventional galvanostatic technique described elsewhere [2, 3]. Briefly, the method involves measuring the gradient of the overpotential/time response of an electrode to a constant current pulse. At sufficiently short times (e.g. 10 μs), in the absence of faradaic reactions, the response curve following the sudden, almost vertical, ohmic overpotential component is linear and the capacitance associated with double layer charging can be calculated from the equation

$$C = I_p\left(\frac{d\upsilon}{dt}\right)^{-1} \quad (1)$$

where C is the differential capacitance (farads), I_p is the pulse current (amperes) and $(d\upsilon/dt)$ is the gradient of the overpotential/time curve (volts/second).

A block diagram of the instrumentation used for capacitance measurements is shown in Fig. 1. A circuit diagram of the IC pulse generator also incorporating the polarizing voltage source is available from the author. The device provided 6 V square pulses having widths from 100 ms to 5 μs (rise times $\sim$ 0·3 μs) either 'single shot' or at a slow repetition rate (1–30 pulses/sec).

The oscilloscope was a Hewlett-Packard type 175A fitted with a dual trace vertical amplifier (1755A) and delay generator (1781B).

The output from the generator was continuously monitored on the upper oscilloscope channel A. This enabled the pulse current to be measured by dividing the pulse amplitude by the value of the series standard resistance R_s (10-100 kΩ). The small voltage drop across the cell was ignored in calculating the pulse current. The response transients were simultaneously dis-

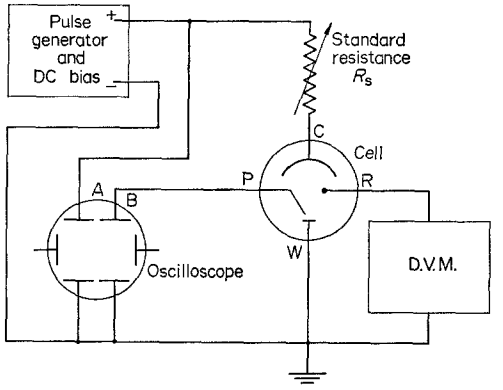

Fig. 1. Electrical circuit for capacitance measurements.

played on the lower channel (B). The pulse current (60–600 μA) was adjusted to give electrode overpotentials in the region 5–30 mV.

Polarizing potentials were measured by means of a DVM (Bradley type 173B).

2.2 *Cell*

The working electrode (W) was placed at the the centre of a helical Pt* wire counter electrode (C). The reference electrode (R), Hg/HgO/10M KOH, was connected to the working compartment by a Luggin capillary via a closed tap. The latter was necessary to eliminate free Hg^{2+} from the working compartment. A fine Pt wire probe (P) placed close to the working electrode enabled transients to be observed down to 1 μs. The electrolyte in the cell was purged with nitrogen before use.

Throughout this investigation potentials are referred to Hg/HgO/10M KOH except where otherwise stated.

2.3 *Test electrodes.*

The Cu and Zn electrodes were 1 mm diameter wires of 99·999% purity encased in tightly fitting p.t.f.e. sleeves. The Sn electrode was similarly fabricated from 5 mm diameter rod of 99·9999% purity. All metals were supplied by Koch-Light Ltd.

* In measurements involving copper working electrodes both nickel and copper counter electrodes were also tried. The results were similar to those obtained where a platinum counter electrode had been used. Thus contamination from dissolved platinum is thought to be insignificant.

The electrodes after being machined flat were abraded (P600A silicon carbide paper) and polished to mirror-like, scratch-free surfaces using successively 14–6, 6–3 and 1–1/4 μ diamond pastes (Metallurgical Services 'Dialap' compound and lubricant). The electrodes were washed well with CCl_4 to remove all traces of polishing lubricant.

2.4 *Mercury doping.*

Microgram quantities of mercury were electrodeposited onto the test electrodes at constant current from 1M KOH saturated with yellow mercuric oxide, according to the method described by Vondrak and Balej [4].

Mercury doped electrodes (particularly Cu) were readily oxidised in air and required rapid manipulation. The electrodeposition and washing procedures were facilitated by a glove box filled with nitrogen (Mecaplex, evacuable type, G-B3011). Solvents were deoxygenated using the freeze-thaw technique. Mercury doped electrodes were sealed in small polythene bags (nitrogen filled) before handling in air.

2.5 *Electrolyte*

The electrolyte (10M KOH) was prepared from nitrogen-saturated triply distilled water and A.R. KOH.

2.6 *Measurements*

In order to prevent damage to its surface, the electrode was always placed in the capacitance cell at potentials more cathodic than its rest potential. The capacitance values invariably decreased slowly with time (probably because of rearrangement of surface atoms), but after equilibration for 20–30 min became stable in the absence of impurities and electrolyte leakage into the electrode mount.

In order to obtain absolute capacitance values at ideally polarizable heterogeneous surfaces, long duration pulses should be employed [3]. In practice this suffers from two major disadvantages. Firstly, the pulse introduced additional faradaic processes which are difficult to distinguish from those already present and secondly,

the inherent trace curvature introduces estimation errors. As this study was on a comparative basis, the longest pulse width consistent with linearity was considered to be the best compromise.

The pulse widths used were between 10 μs and 1 ms. Families of capacitance curves for a particular metal were always obtained at the same pulse width.

Triggering the pulse generator electronically at a slow repetition rate (10 pulses/second) was found to be more convenient than 'single shot' operation because it enabled measurements to be made without photographic means. Provided the repetition rate was made sufficiently slow so that the double layer relaxed completely between pulses, the results were identical to those obtained by the 'single shot' technique [2].

3. Results and discussion

3.1 *Copper*

The family of capacitance curves for copper doped with progressively increasing concentrations of Hg, in 10M KOH, are shown in Fig. 2. The curve for pure copper is similar to that recently reported by Hampson *et al* [5]. The overpotential-time transients even for highly polished copper showed extreme curvature at longer pulse times (>1 ms) which may be due to faradaic processes and/or surface heterogeneity. This is also reflected by the high values for the capacitance minima ($\sim$50 μF cm^{-2}) even at relatively short pulse times (10 μs). A high degree of frequency dispersion for copper in NaOH was similarly observed by Hampson *et al.* [5].

The first pseudo-capacitance peak at $\sim -0{\cdot}45$ V arises from chemisorption of OH^- followed by charge transfer to yield copper (I) oxide or hydroxide at the electrode surface. A dark passivating oxide film was observed to form at $-0{\cdot}3$ V and its low dielectric constant would account for the sharp decrease in capacitance ($\sim$ 8 μF cm^{-2}).

The second peak at $-0{\cdot}88$V may correspond with that observed at $-0{\cdot}65$V NHE by other workers for copper in alkaline [5] and neutral salt [6, 7] solutions, which is thought to be due to adsorbed hydrogen. This type of behaviour has been well-established for a number of transition metals such as Fe [8], Ni [9] and Pt [10].

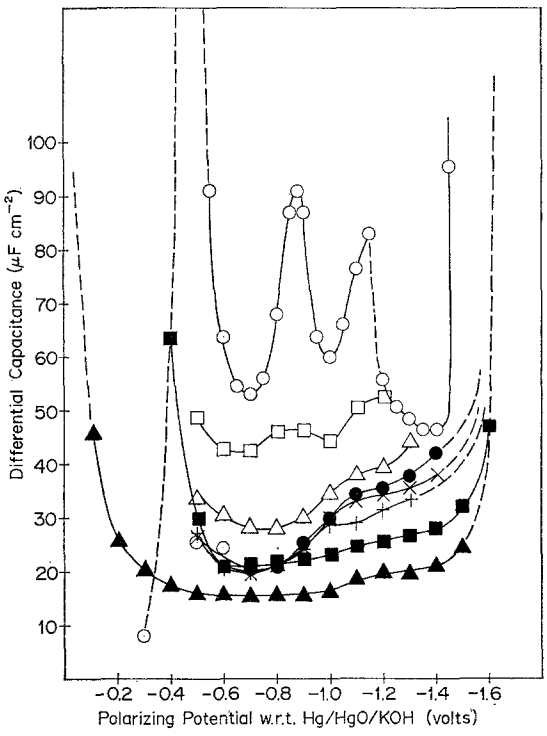

Fig. 2. Capacitance curves for copper, mercury and mercury-doped copper in 10M KOH. Pulse width 10 μs. (○) Cu only (□) 1 μg cm^{-2} Hg (△) 2 μg cm^{-2} Hg (●) 4 μg cm^{-2} Hg (×) 10 μg cm^{-2} Hg (+) 100 μg cm^{-2} Hg (■) 41 mg cm^{-2} Hg (▲) Hg only (DME).

The third peak or discontinuity at $-1{\cdot}15$V coincided with the nucleation of hydrogen bubbles. The capacitance value at $-1{\cdot}2$V dropped slowly with time but after about 5 min. became fairly constant over the range $-1{\cdot}2$ to $-1{\cdot}4$V. Above $-1{\cdot}4$V the very rapid evolution of hydrogen was accompanied by a sudden increase in capacitance (curved transients).

On examination of the curves for mercury doped copper it is apparent that extremely small quantities of mercury (1–10 μg cm^{-2}) markedly decrease the capacitance values by removing the pseudo-capacitance components due to hydrogen adsorption.

Polarization studies [4] have shown that similar 'monolayer' concentrations of mercury are sufficient to inhibit the hydrogen evolution reaction on a number of transition metal surfaces.

The response transients for copped doped with as little as 10 μg cm^{-2} of mercury showed considerably reduced curvature at longer pulse

times (up to 1 ms) confirming the reduced surface heterogeneity. However, the frequency dispersion effect was only completely absent for copper covered by relatively thick, liquid films of mercury (~40 mg cm^{-2}). The respective capacitance curve, as might be expected, closely resembles that obtained [11] for a dropping mercury electrode (DME) in 1,5 and 10M KOH, except that oxidation occurs at less anodic potentials (~ −0·4 V) than pure mercury (+38 mV) because of the small quantity of dissolved copper in the film. The double layer behaviour of mercury in 1 and 10M NaOH has been investigated in detail by Armstrong *et al* [12]. As might be expected the Hg/NaOH and Hg/KOH systems are very similar.

The cathodic branch of the capacitance curve for mercury in 10M KOH is given in Fig. 2 for comparison purposes. It is interesting to note that the cathodic minimum for mercury in 10M KOH is close (±0·8 $\mu F\ cm^{-2}$) to the value of 16 $\mu F\ cm^{-2}$ obtained for mercury [3] in a number of dilute aqueous electrolytes. There is no evidence for specific adsorption of OH^- in the potential region −0·2 to −1·5 V.

3.2 *Tin*

The transients observed for highly polished tin showed only slight curvature (low surface heterogeneity) at longer pulse times. They were almost linear up to 1 ms. Polycrystalline tin in perchlorate electrolytes is similarly reported [13] to show little dispersion of capacitance with frequency.

The family of capacitance curves for tin and mercury doped tin are shown in Fig. 3. The steep anodic rise in capacitance at potentials below −1·1 V arose from lattice dissolution probably preceded by adsorption of OH^-. Hydrogen bubbles were observed on the electrode at potentials above −1·3 V.

Tin can be classified [14] with the metals Ga, Bi and Pb as being 'mercury like' with respect to its double layer behaviour. It should exhibit low surface heterogeneity and have little tendency to adsorb hydrogen. This is apparent from the results of the present investigation.

In contrast to copper, the addition of 10 $\mu g\ cm^{-2}$ Hg produced little change in the capacitance curve for tin, apart from a slight shift in

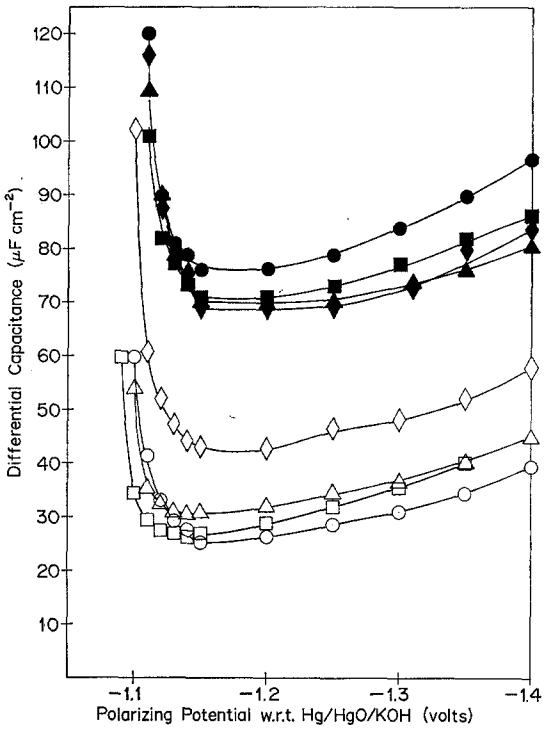

Fig. 3. Capacitance curves for tin and mercury-doped tin in 10M KOH. Pulse width 850 μs. (○) Sn only, (□) 10 $\mu g\ cm^{-2}$ Hg, (△) 100 $\mu g\ cm^{-2}$ Hg, (◇) 250 $\mu g\ cm^{-2}$ Hg, (●) 500 $\mu g\ cm^{-2}$ Hg, (■) 600 $\mu g\ cm^{-2}$ Hg, (▲) 750 $\mu g\ cm^{-2}$ Hg, (◆) 1 mg cm^{-2} Hg.

potential of the cathodic minimum. Addition of larger quantities of mercury caused a striking three-fold increase in capacitance, the effect being a maximum at about 500 $\mu g\ cm^{-2}$ Hg. Little further change (possibly a slight decrease in capacitance) was observed in the range 500 $\mu g\ cm^{-2}$ to 1 mg cm^{-2} Hg.

The increase in capacitance is probably best interpreted as being due to increased surface roughness. Electrodeposition of mercury (2 mg cm^{-2}) on silver is reported [15] to have a similar effect. The roughening is probably best envisaged as arising from the localized dissolution at the tin intercrystalline grain boundaries by mercury. The effect is not observed in the case of copper, presumably because of its very much lower solubility [16] in mercury (0·0032 wt % at ~25°C) compared with tin (0·62 wt % at ~25°C).

3.3 *Zinc*

The response transients for polycrystalline zinc

showed a moderate degree of curvature, but were fairly linear up to 100 μs.

The capacitance curves for zinc and mercury doped zinc are shown in Fig. 4. The double layer region for zinc in alkaline solution is complicated by two large pseudo-capacitance components arising from lattice dissolution below $-1{\cdot}4$ V and hydrogen evolution above $-1{\cdot}5$ V. The capacitance minimum between $-1{\cdot}5$ and $-1{\cdot}55$ V is considered [3] to be a true cathodic minimum even though it is just on the point of hydrogen evolution. It has been used as such for the measurement of real surface areas of porous zinc electrodes.

Like tin, the capacitance minima for zinc increase with increasing mercury concentration, reaching a maximum at about 100 μg cm^{-2}. Little further change was produced in the range 100 to 500 μg cm^{-2} Hg. By analogy with tin, mercury at low surface concentration appears to increase the roughness of the zinc surface, again probably by attack at the intercrystalline grain boundaries. The solubility [16] of zinc in mercury is appreciable, being 2·15 wt % at ~25°C. The reported decrease in capacitance for amalgamated zinc electrodes [17] was only observed in the present investigation at extremely high mercury concentrations (~100 mg cm^{-2}) where a visible film of free liquid mercury was present.

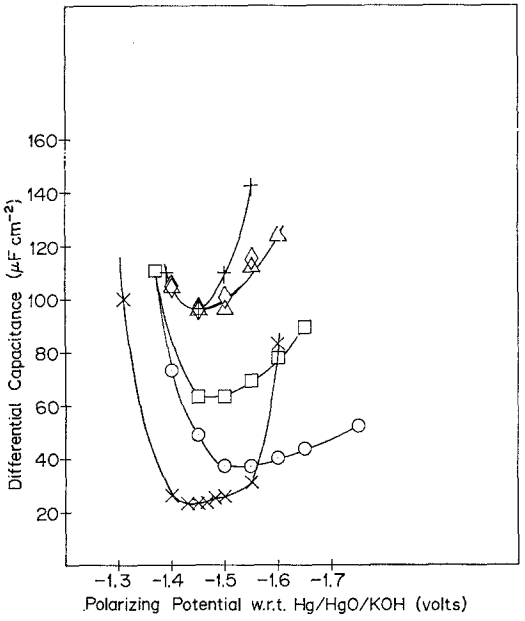

Fig. 4. Capacitance curves for zinc and mercury-doped zinc in 10M KOH. Pulse width 100 μs. (○) Zn only, (□) 10 μg cm^{-2} Hg, (△) 100 μg cm^{-2} Hg (◇) 250 μg cm^{-2} Hg, (+) 500 μg cm^{-2} Hg, (×) 100 mg cm^{-2} Hg.

The reduction in capacitance at amalgamated zinc electrodes in alkaline solution is generally interpreted in terms of reduced OH^- adsorption [17, 18, 19]. However, in the light of the present investigation the results could equally well be interpreted as a decrease in surface roughness.

A factor often ignored in dealing with amalgamated polycrystalline electrodes is diffusion of mercury from the surface into the bulk metal. Although diffusion of mercury through the lattice is a very slow process, diffusion of mercury down the grain boundaries is relatively fast [20]. This becomes of particular importance in considering the long-term storage of battery anodes.

Thus, in dealing with polycrystalline metals which are appreciably soluble in mercury, such as tin and zinc, unless the concentration of mercury at the surface is carefully specified it cannot be assumed that amalgamation necessarily produces a smooth mercury-like surface.

Acknowledgement

The author wishes to thank the Directors of the Ever Ready Co. (G.B.) Ltd., for permission to publish this work.

References

[1] T. P. Dirkse, 6th International Power Sources Symposium, 1968. Paper 26; p. 353.
[2] J. S. Riney, G. M. Schmid and N. Hackerman, *Rev. Sci. Instr.*, **32** (1961) 588.
[3] R. A. Myers and J. M. Marchello, *J. Electrochem. Soc.*, **116** (1969) 790.
[4] J. Vondrak and J. Balej, *Electrochim. Acta.* **15,** (1970) 1653.
[5] N. A. Hampson, R. J. Latham, J. B. Lee and K. I. Macdonald, *J. Electroanal. Chem.*, **31** (1971) 57.
[6] D. Armstrong, N. A. Hampson, and R. J. Latham, *J. Electroanal. Chem.*, **23** (1969) 361.
[7] P. Champoin, G. Grespy and J. Royon. *C. R. Acad. Sci. Ser. C.*, **270** (1970) 1552.
[8] B. B. Damaskin, O. A., Petrii and V. V. Batrakov, 'Adsorption of Organic Compounds on Electrodes', Plenum Press, New York, London (1971) p. 291.

[9] J. L. Weininger and M. W. Breiter, *J. Electrochem. Soc.*, **111** (1964) 707.
[10] See [8] p. 409.
[11] R. Barnard and J. A. Lee, Unpublished results.
[12] R. D. Armstrong, W. P. Race and H. R. Thirsk, *J. Electroanal. chem.*, **19** (1968) 233.
[13] N. A. Hampson and D. Larkin, *J. Electrochem. Soc.*, **115** (1968) 612.
[14] See [8] p. 231.
[15] See [8] p. 244.
[16] N. V. Sidgwick, 'The Chemical Elements and their Compounds', Clarendon Press, Oxford (1950) Vol. 1, p. 289.
[17] T. P. Dirkse and R. Shoemaker, *J. Electrochem. Soc.*, **115** (1968) 784.
[18] N. A. Hampson, Chapter 5 in 'Zinc–Silver Oxide Batteries', Ed. A. Fleischer and J. J. Lander, J. Wiley and Sons, New York, London, Sydney, Toronto, (1971) p. 59–61.
[19] R. D. Armstrong, G. M. Bulman and H. R. Thirsk, *J. Electroanal. Chem.*, **22** (1969) 55.
[20] F. L. Tye, J. T. Williams and J. Swift, 'Amalgamation of Zinc Anodes in Leclanche Dry Cells', paper No. 16 to be presented at the 8th International Power Sources Symposium 1972.